MCP-1/CCR2 axis inhibits the chondrogenic differentiation of human nucleus pulposus mesenchymal stem cells

XUANCHENG OU[1], TIANYONG WEN[2], JINWEI YING[3], QING HE[2], ANWU XUAN[2,4] and DIKE RUAN[2,4]

[1]Department of Spine Surgery, The Central Hospital of Yongzhou, Yongzhou, Hunan 425000; [2]Department of Orthopedic Surgery, The Sixth Medical Centre of PLA General Hospital, Beijing 100053; [3]Department of Orthopedic Surgery, The First Affiliated Hospital of Wenzhou Medical University, Wenzhou, Zhejiang 325000; [4]The Second School of Clinical Medicine, Southern Medical University, Guangzhou, Guangdong 510515, P.R. China

Received April 16, 2021; Accepted November 15, 2021

DOI: 10.3892/mmr.2022.12793

Abstract. Intervertebral disc degeneration (IDD) creates a hostile environment with high osmotic pressure, high mechanical stress, hypoxia and a low pH, where cytokines such as TNF-α and IL-1β are highly expressed. The degenerating intervertebral disc has high local expression of monocyte chemoattractant protein-1 (MCP-1), which is associated with the degree of degeneration. However, there are a few reports on the influence of MCP-1 on nucleus pulposus-derived stem cells (NPSCs). In the present study, a significant upregulation of MCP-1 was observed in NPSCs cultured *in vitro* with pro-inflammatory cytokines. MCP-1 significantly inhibited the migration and proliferation of NPSCs in a dose-dependent manner as detected via Cell Counting Kit-8, wound healing and Transwell assays. Western blotting and histological analysis demonstrated that MCP-1 significantly reduced chondrogenic NPSC differentiation. Reverse transcription-quantitative PCR and western blotting revealed that C-C chemokine receptor type 2 (CCR2) mRNA and protein expression levels were significantly enhanced by MCP-1. Furthermore, MCP-1 significantly inhibited the migration, differentiation and proliferation of NPSCs, which was effectively reversed by blocking CCR2 with the inhibitor RS504393. Overall, these results demonstrated that MCP-1 may contribute to the inhibition of chondrogenic NPSC differentiation via MCP-1/CCR2 chemotaxis signals, providing a potential therapeutic target for IDD.

Correspondence to: Dr Dike Ruan, The Second School of Clinical Medicine, Southern Medical University, 1023 South Shatai Road, Guangzhou, Guangdong 510515, P.R. China
E-mail: ruandikenghh@163.com

Abbreviations: IDD, intervertebral disc degeneration; MCP-1, monocyte chemoattractant protein-1; NPSCs, nucleus pulposus-derived stem cells

Key words: IDD, NPSCs, MCP-1, C-C chemokine receptor type 2

Introduction

Intervertebral disc degeneration (IDD) is a major cause of degenerative spine diseases, such as cervical spondylosis, spinal column stenosis and intervertebral disc herniation (1,2). Current treatments for such diseases include conservative treatment and surgery. Conservative treatments for this condition include rest, administration of anti-inflammatory and analgesic drugs, or combined physiotherapy (3-5) However, their disadvantages include the need for early intervention, recurrent symptoms and failure of radical treatment. Surgical treatments include nucleus pulposus removal, discectomy and fusion (6,7). Although short- and medium-term efficacy is satisfactory after surgery, complications, such as adjacent segment degeneration, may occur during long-term follow-up (8). Therefore, there is currently no effective treatment for this disease. Although conventional methods may relieve local symptoms, they are insufficient to properly treat IDD; thus, the normal physiological structure and function of the intervertebral disc are not recovered (9). Therefore, novel treatments are urgently needed to treat IDD.

At present, the pathogenesis of IDD remains unclear. The major pathological changes of the disease are characterized by a decrease in the number and function of nucleus pulposus cells, as well as extracellular matrix degradation (1,10). Under normal conditions, nucleus pulposus cells secrete a large amounts of proteoglycans, collagen-II and other extracellular matrix proteins, to maintain the elasticity and the load-bearing balance of the intervertebral disc (11). Under pathological conditions, fewer nucleus pulposus cells, decreased matrix secretion and stress changes in the intervertebral disc result in degradation, ultimately contributing to intervertebral disc protrusion, spinal column stenosis and spinal instability (12,13).

Among the biological therapies for IDD, mesenchymal stem cells show great potential in IDD recovery due to their ability to self-replicate and differentiate into numerous cell lineages (14). In previous studies (15,16), it was observed that nucleus pulposus-derived stem cells (NPSCs) are important for maintaining the normal function and homeostasis of the

nucleus pulposus. Another study reported that the differentiation of NPSCs is weakened in the elderly and individuals with a degenerative condition (17). Therefore, an ideal therapeutic approach would be to activate NPSCs to differentiate into nucleus pulposus-like cells for the self-healing of tissues. However, little is known about the influencing factors and specific mechanisms of NPSC degeneration or the functional inhibition of the intervertebral disc microenvironment. Therefore, clarifying the influencing factors and mechanism of degeneration of NSPCs in the intervertebral disc microenvironment, in order to restore their biological performance, is important for IDD treatment.

The degenerating intervertebral disc is considered to be a complex and harsh microenvironment, characterized by hypoxia, inflammation, high osmotic pressure and high mechanical stress. These complex factors in the microenvironment affect the activity of cells in the disc (18). The injured intervertebral disc can secrete various cytokines or chemokines, induce endogenous stem cells in the surrounding tissue stem cell nests to migrate to the lesion site, and promote endogenous repair and regeneration (19,20). Previous studies on the locally expressed cytokines in IDD have mainly focused on TGF-β, TNF-α, IL-1β and monocyte chemoattractant protein-1 (MCP-1) (21-23). In certain studies, IDD has been reported to be associated with high local expression levels of MCP-1, which may be associated with the degree of IDD (24,25). However, relevant reports outlining the role of MCP-1 in IDD are rare.

Current studies regarding mesenchymal stem cells and MCP-1 have focused on promoting the migration of endogenous neural stem cells to improve neurofunctional repair and to promote the homing of bone marrow stem cells post-myocardial infarction to enhance recovery. These studies have also investigated their roles in human immunoregulation and the promotion of wound healing (26-28). The functions of MCP-1 were mainly realized via binding to its specific receptor, C-C chemokine receptor type 2 (CCR2) (29). The MCP-1/CCR2 signaling axis has extensive biological effects and has been reported to be important in immunodeficiency diseases, implant-related immune responses and in tumors (17). However, there are few reports on the local role of MCP-1 in IDD (30). The present study aimed to determine whether the upregulation of MCP-1 in IDD could enhance endogenous regeneration in the intervertebral disc by regulating the differentiation of NPSCs to IDD stem niches. To the best of our knowledge, the present study was the first to reveal the role of the MCP-1/CCR2 axis in the chondrogenic NPSC differentiation at the injury site of IDD.

Materials and methods

NPSC isolation from primary cultures. The NPSCs used in the present study were collected from a 16-year-old female patient with trauma-induced intervertebral disc protrusion. The patient's parents provided written consent for the collection and use of her vertebral tissue. This research was approved by the Ethics Committee of the Second School of Clinical Medicine, Southern Medical University (Guangzhou, China; approval no. ICE2017058). Under sterile conditions, the isolated human nucleus pulposus was washed twice with PBS, separated carefully from the surrounding tissue, cut into 0.5x0.5x0.5-mm cubes and placed into a 0.02% collagenase II solution. The tissue was digested in an incubator at 37˚C with 5% CO_2 for 4 h. A sterile steel wire mesh (200 μm) was used to filter the tissue fragments. The resulting cell suspension was centrifuged at 800 x g for 5 min at 4˚C. The supernatant was discarded and the cells were collected. The cells were then cultured in DMEM/F12 (cat. no. 12400024; Thermo Fisher Scientific, Inc.) medium containing 10% fetal bovine serum (FBS; cat. no. 16140071; Thermo Fisher Scientific, Inc.) and 1% penicillin/streptomycin in an incubator at 37˚C with an atmosphere of 5% CO_2. After 2 weeks of static culture, the cells adhered to the culture vessel and the spent culture medium was replenished every 2-3 days. Subculturing was performed when the cells reached 80-90% confluence. During subculturing, a trypsin solution (cat. no. C0204; Beyotime Institute of Biotechnology) was used to dissociate the cells for 3 min. The cells were then seeded into culture flasks at a density of $5x10^3$ cells/cm^2. After the cells reached P2 generation with 80-90% confluence, NPSCs were obtained.

NPSC sorting via flow cytometry. Adherent NPSC cultures at the P2 generation were dissociated using a trypsin solution when they reached 80-90% confluence. The cell suspensions were centrifuged at 800 x g for 5 min at 4˚C to collect the cells. After pelleting the cells, phycoerythrin (PE)-CD73 (1:500; cat. no. ab157335), PE-CD34 (1:500; cat. no. ab223930), peridinin-chlorophyll-protein-CD45 (1:500; cat. no. ab210221), allophycocyanin-CD90 (1:500; cat. no. ab272351) and FITC-CD105 (1:500; cat. no. ab53318) antibodies (all purchased from Abcam) were added and the cell suspension was incubated for 30 min at 4˚C in the dark. Subsequently, the cells were centrifuged again at the aforementioned parameters and washed twice with PBS containing 4% FBS. A MoFlo High-Speed Flow Cytometer (Beckman Coulter, Inc.) with Summit software (version 62; Beckman Coulter, Inc.) was used to sort $CD34^+$, $CD45^+$, $CD73^+$, $CD90^+$ and $CD105^+$ cells. The sorted NPSCs were seeded into culture dishes at a density of $5x10^3$ cells/cm^2 for further culture. The cells were cultured in an incubator with 5% CO_2 at 37˚C for 2 weeks before subsequent experimentation.

Observation of cell morphology. Sorted NPSCs were seeded into a culture flask at a density of $5x10^3$ cells/cm^2 to observe the cell morphology using a light microscope (Olympus Corporation). The morphological characteristics of the sorted NPSCs were recorded 4-6 h after seeding.

Induced differentiation potential of isolated NPSCs. Osteogenic (cat. no. Rasmx-90021.), adipogenic (cat. no. Rasmx-90031) or chondrogenic (cat. no. Rasmx-90041) (all Cyagen Biosciences, Inc.) medium was applied to induce three different differentiated lines of NPSCs for ~2 weeks at 37˚C. After fixing cells with 4% neutral formaldehyde solution for 30 min at room temperature, Alizarin Red (3-5 min; room temperature), Oil Red O (30 min; room temperature) and Alcian Blue (30 min; room temperature) staining were used to determine the osteogenic, adipogenic and chondrogenic differentiation capacities of the three NPSC lines, respectively.

Images were captured using a light microscope (Olympus Corporation).

Synthesis and expression of MCP-1 in a pro-inflammatory environment. NPSCs ($1x10^5$ cells/well) were plated in 6-well plates and cultured in complete medium for 1 day. To simulate the proinflammatory and poor nutrition microenvironment of the degenerative disc, the medium was then replaced with serum-free medium (SFM) comprising low glucose-DMEM and 10 ng/ml interleukin (IL)-1β (PeproTech, Inc.) or 50 ng/ml tumor necrosis factor-α (TNF-α; PeproTech, Inc.). After 48 h of incubation at 37˚C, the protein levels of MCP-1 secreted in the culture medium were quantified using an enzyme-linked immunosorbent assay (ELISA) kit for monocyte chemotactic protein 1 (MCP1; cat. no. SEA087Hu; Wuhan USCN Business Co., Ltd.) according to the manufacturer's instructions. Total RNA was extracted using TRIzol® reagent (Invitrogen; Thermo Fisher Scientific, Inc.) followed by the quantification of MCP-1 mRNA expression levels via reverse transcription-quantitative PCR (RT-qPCR).

Cell proliferation assay. The Cell Counting Kit-8 kit (Dojindo Molecular Technologies, Inc.) was applied for the detection of cell proliferation. NPSCs in the P3 generation growing in the logarithmic phase were seeded into a 96-well plate at a density of $1x10^4$ cells/ml. With triplicate wells for each group, 100 µl cell suspension was added to each well and incubated overnight in a thermostatic incubator with 5% CO_2 at 37˚C. The next day, the spent medium was replaced with a medium containing different concentrations of MCP-1 (0, 10, 50 and 100 ng/ml; cat. no. SRP3109; Merck KGaA) with or without RS504393 treatment for 1, 3, 5 and 7 days of stimulation at 37˚C. Subsequently, 10 µl CCK-8 solution was added into each well and an equivalent amount of CCK-8 solution was added into the cell-free well. Cells were then incubated for 2 h at 37˚C in the dark. A microplate reader was used to measure the optical density (OD) at 450 nm. The final OD value was obtained by subtracting the OD value of the blank well from that of each experimental well. Air bubbles were carefully avoided while adding liquids to the culture as they could affect the OD measurement.

Wound healing assay. NPSCs were seeded into 6-well plates at a density of $5x10^4$ cells/ml and were cultured to ~100% confluence. A 200-µl pipette tip was used to create a straight wound by disrupting the monolayer. After the cells were washed with PBS twice, SFM containing 0, 10, 50 and 100 ng/ml MCP-1 was added and the cells were incubated for another 12 h at 37˚C to allow them to migrate back into the wound area. For the inhibition experiment, the cells were pre-treated with 10 µg/ml RS504393 (cat. no. SML0711; Merck KGaA) for 2 h at 37˚C, followed by incubation with 50 or 100 ng/ml MCP-1 at 37˚C. To assess the mean number of migrated cells, low-power fields were randomly selected from each group for cell counting. Images were captured by using a light microscope (Olympus Corporation).

Transwell migration assay. Transwell 24-well chamber plates (Costar; Corning, Inc.) with a pore size of 8 µm, were employed for the migration assay. In each well, 200 µl SFM containing $1x10^5$ cells and 600 µl SFM containing 10% serum supplemented with 0, 10, 50 or 100 ng/ml MCP-1 were placed into the upper and lower chambers, respectively. For the inhibition experiment, the cells were pre-treated with 10 µg/ml RS504393 for 2 h at 37˚C before being added to the upper chamber. After 12 h of incubation at 37˚C, the cells that adhered on the upper side of the membrane were gently removed with a cotton swab and cells on the underside were fixed with 4% paraformaldehyde fix solution (cat. no. P0099; Beyotime Institute of Biotechnology) for 0.5-1 h at room temperature and stained with 0.1% crystal violet for 0.5-1 h at room temperature. The mean number of cells from three random high-power fields under a light microscope (Olympus Corporation) was assessed to measure cell migration.

Cell cycle detection via flow cytometry. NPSCs in the P3 generation growing in the logarithmic phase were seeded into 6-well plates at a density of $5x10^5$ cells/ml. Cells were cultured in a thermostatic incubator for 24 h to synchronize their cell cycles. The spent medium was replaced with SFM to create a starved culture and the cells were cultured overnight. After 72 h, complete medium containing different concentrations (0, 10, 50 or 100 ng/ml) of MCP-1 was added for 24-48 h at 37˚C. To the collected cells, 1 ml pre-cooled 70% ethanol solution was added into each tube and after mixing, the solution was stored in the refrigerator overnight at 4˚C. Following centrifugation (300 x g, 10 min, 4˚C) and careful removal of the supernatant, 1 ml pre-cooled PBS was added and the cells were re-suspended, followed by further centrifugation (1,000 x g, 4˚C, 10 min) and removal of the supernatant under direct visualization. Then RNase A (100 µl; cat. no. EN0531; Thermo Fisher Scientific, Inc.) was used to treat cells. Freshly prepared propidium iodide (PI) staining solution (500 µl) weas used to re-suspend the cells. After soaking in a water bath at 37˚C for 30 min in the dark, the cell suspension was rapidly stored on ice for flow cytometry. Finally, the flow cytometer (BD FACSAria III Flow Cytometer; BD Biosciences) was used to detect the red fluorescence intensity at an excitation wavelength of 488 nm and light scattering was detected for the analysis of cell DNA content using CELL QUEST analysis software (version 3.3; BD Biosciences).

Annexin V-FITC/PI staining analysis via flow cytometry. The Annexin V-FITC/PI apoptosis detection kit (cat. no. 40302ES20; Shanghai Yeasen Biotechnology Co., Ltd.) was used. NPSCs in the P3 generation were seeded ($1x10^6$) into a culture flask and the spent medium was replaced after overnight incubation at 37˚C. Different concentrations (0, 10, 50 or 100 ng/ml) of MCP-1 were then added to the cells, which were incubated for 72 h at 37˚C. The cells in each group were then collected, washed with 1 ml binding buffer, centrifuged at 800 x g for 10 min at 4˚C and the supernatant was discarded. After the cells were resuspended using 100 µl binding buffer, 10 µl Annexin V-FITC was added, followed by 15 min of incubation at room temperature (20-28˚C) in the dark. After washing with 1 ml binding buffer, the cell suspension was centrifuged at 800 x g for 10 min at 4˚C and the supernatant was discarded. Binding buffer (500 µl) was then added to resuspend the cells, followed by the addition of 5 µl PI solution for 10-15 min at room temperature. The cells were

immediately subjected to flow cytometry (BD FACSAria III Flow Cytometer; BD Biosciences). Annexin V-positive cells represented early apoptosis, PI-positive NPSC cells represented late apoptosis, and Annexin V- and PI-positive cells represented necrosis. CELL QUEST analysis software (version 3.3; BD Biosciences) were used to analyze cell apoptosis.

MCP-1-induced chondrogenic differentiation of NPSCs. NPSCs were cultured for 72 h in a complete culture medium containing MCP-1 (0, 50 and 100 ng/ml) with or without 2 h of pre-treatment with 10 μg/ml RS504393 at 37˚C for 24-48 h. Prior to western blotting, total protein was extracted using RIPA lysis buffer (Applygen Technologies, Inc.) containing PMSF. Total RNA was extracted using TRIzol reagent. The aggregate chondrogenesis model was constructed by centrifuging NPSCs (300 x g, 4˚C, 5-10 min) into cell micromasses and inducing chondrogenic medium. MCP-1 was added to complete chondrogenic medium (Cyagen Biosciences, Inc.) to determine whether MCP-1 contributes to TGF-β1-induced NPSC chondrogenesis. An inhibition assay was then performed via treatment with 10 μg/ml RS504393 (a CCR2 antagonist) at 37˚C for 24-48 h. Aggregates were collected for histological analysis after 28 days.

Immunohistochemical analysis. Cartilage samples were fixed with 4% paraformaldehyde fix solution (cat. no. P0099; Beyotime Institute of Biotechnology) for 0.5-1 h at room temperature. Paraffin-embedded samples were then serially prepared into 5-μm-thick sagittal disc sections and then deparaffinized in dimethylbenzene (three times; each 8 min) followed by rehydration with an alcohol gradient. Subsequently, samples were incubated overnight at 4˚C with primary antibodies targeted against: Collagen-II (1:200; cat. no. ab34712; Abcam) and aggrecan (1:400; cat. no. bs-11655R; BIOSS). After washing with PBS, samples were incubated with a horseradish peroxidase-conjugated goat anti-rabbit IgG secondary antibody (1:200; cat. no. ab6721; Abcam) for 20 min at 37˚C. Color development was then performed using DAB (Beyotime Institute of Biotechnology) for 5 min at room temperature. Subsequently, the sections were counterstained with hematoxylin at room temperature for 2 min (Beyotime Institute of Biotechnology), mounted on coverslips and observed under a light microscope (Nikon Corporation). ImageJ software (version 1.8.0; National Institutes of Health) was used for quantification.

RT-qPCR. Total RNA was isolated from cultured cells using TRIzol® reagent (Invitrogen; Thermo Fisher Scientific, Inc.). cDNA was synthesized from 1 μg total RNA using the GoScript™ Reverse Transcription System (Promega Corporation) according to the manufacturer's instructions. qPCR was performed using a LightCycler® 480 Real-Time PCR System with SYBR Green Master I (Roche Diagnostics). With a 20-μl reaction volume, the reactions were run on a Peltier Thermal Cycler (Bio-Rad, Laboratories, Inc.). The following thermocycling conditions were used for qPCR: Initial denaturation at 95˚C for 5 min; followed by 40 cycles at 95˚C for 10 sec of denaturation, 60˚C for 20 sec of annealing and elongation; and 72˚C for 20 sec of final extension. The custom-made primers (Sangon Biotech, Shanghai, China) are presented in Table I. Relative mRNA expression levels were quantified using the $2^{-\Delta\Delta Cq}$ method and normalized to the internal reference gene, GAPDH (31).

Table I. Sequences of primers used for reverse transcription-quantitative PCR.

Gene	Sequence (5'-3')
CCR2	F: TGCTCCCTGTCATAAA
	R: AGATGAGGACGACCAGCAT
Collagen-II	F: TGGACGATCAGGCGAAACC
	R: GCTGCGGATGCTCTCAATCT
Aggrecan	F: GTGCCTATCAGGACAAGGTCT
	R: GATGCCTTTCACCACGACTTC
SOX-9	F: AGCGAACGCACATCAAGAC
	R: CTGTAGGCGATCTGTTGGGG
MCP-1	F: CAGCCAGATGCAATCAATGCC
	R: TGGAATCCTGAACCCACTTCT
GAPDH	F: GGAGCGAGATCCCTCCAAAAT
	R: GGCTGTTGTCATACTTCTCATGG

CCR2, C-C chemokine receptor type 2; MCP-1, monocyte chemoattractant protein-1; F, forward; R, reverse.

Western blotting. Protein concentrations were determined using the BCA Protein Assay kit (Beyotime Institute of Biotechnology). Total protein samples (40 μg protein/lane) were separated via SDS-PAGE on 8 or 10% gels and then transferred onto polyvinylidene fluoride membranes (MilliporeSigma). The membranes were then blocked using 5% skimmed milk in TBS containing 0.05% Tween-20 for 2 h at 37˚C. Subsequently, membranes were incubated with primary antibodies against CCR2 (1:1,000; cat. no. ab203128; Abcam), GAPDH (1:10,000; cat. no. ab8245; Abcam), aggrecan (1:1,000; cat. no. 13880-1-AP; ProteinTech Group, Inc.), SOX-9 (1:1,000; cat. no. ab185966; Abcam) and collagen-II (1:1,000; cat. no. ab34712; Abcam) overnight at 4˚C. The membranes were then incubated for 1 h with horseradish peroxidase-conjugated secondary antibodies (1:1,000; cat. nos. ab6789 and ab6721; Abcam) at room temperature. Using Pierce ECL Western Blotting Substrate (Thermo Fisher Scientific, Inc.) the membranes were visualized using ImageQuant LAS4000 (GE Healthcare). Image-Pro Plus software (version 6.0; Media Cybernetics, Inc.) was used to semi-quantify relative protein expression levels, with GAPDH serving as the loading control.

Statistical analysis. All experiments were repeated at least three times. Data are presented as the mean ± SD. All statistical analyses were conducted using SPSS 22.0 software (IBM Corp.). For normally distributed data, the statistical difference among multiple groups (including the control, IL-1β, TNF-α and IL-1β + TNF-α; control, 10, 50 and 100 ng/ml; and control, 50, 100 and 100 ng/ml + RS504393 groups) was evaluated using one-way ANOVA followed by

Tukey's post hoc test. For non-normally distributed data, the statistical difference was evaluated using the Kruskal-Wallis test followed by the post hoc Dunn test. $P<0.05$ was considered to indicate a statistically significant difference.

Results

Characterization of NPSCs. Primary cells exhibited a representative fibroblast-like morphology within 24 h of incubation (Fig. 1A). The multilineage differentiation assays demonstrated that after specific differentiation induction, isolated cells smoothly differentiated into adipogenic, chondrogenic and osteogenic lineages (Fig. 1B-D). Subsequently, specific cell surface markers commonly used for MSC identification were detected via flow cytometry. Positive results were observed for the commonly used MSC markers CD73 and CD90, as well as CD105, which is expressed in certain MSCs as an auxiliary receptor for the TGF-β receptor complex. Negative results were observed for the hematopoietic markers CD34 and CD45 (Fig. 1E).

MCP-1 expression levels and secretion in an IDD microenvironment. Following treatment with pro-inflammatory cytokines, the mRNA expression levels and protein levels of MCP-1 in NSPCs were examined using RT-qPCR and ELISA, respectively. As Fig. 2A and B shown, MCP-1 was upregulated after being treated with IL-1β or TNF-α and was more upregulated when treated with IL-1β + TNF-α To explore the effect of MCP-1 on NPSC migration and proliferation *in vitro*, Transwell and wound healing and CCK-8 assays were carried out. NPSC migration and proliferation were significantly reduced via MCP-1 treatment in a dose-dependent manner (Fig. 2C-E). Flow cytometry results determined that MCP-1 treatment inhibited the cell cycle in a dose-dependent manner, whereas apoptosis of NPSCs was not affected (Fig. 2F and G).

MCP-1/CCR2 axis regulates the proliferation and migration of NPSCs. As indicated by the results of RT-qPCR and western blotting, MCP-1 significantly enhanced CCR2 mRNA and protein expression levels compared with in the control group; notably, CCR2 upregulation was significantly reversed by the CCR2-specific inhibitor RS504393 compared with the 100 ng/ml MCP-1 group (Fig. 3A and B). As presented in Fig. 3C, the suppressive effect of MCP-1 on cell proliferation was significantly recovered by the CCR2-specific inhibitor RS504393 compared with in the 100 ng/ml MCP-1 group. Similarly, wound healing and Transwell migration assays also revealed that the suppressive effects of MCP-1 on cell migration were significantly reversed by RS504393 compared with in the 100 ng/ml MCP-1 group (Fig. 3D and E).

MCP-1/CCR2 axis regulates the chondrogenic differentiation of NPSCs. To analyze the role of the MCP-1/CCR2 axis in chondrogenic NPSC differentiation *in vitro*, the effect of a CCR2 antagonist on the regulation of cartilage differentiation by MCP-1 at the mRNA and protein levels was determined. Western blotting indicated that MCP-1 suppressed chondrogenic NPSC differentiation, which was manifested through the significantly lower protein expression levels of aggrecan, collagen-II and SOX-9 compared with the control. Furthermore RT-qPCR demonstrated that MCP-1 significantly reduced the mRNA expression levels of aggrecan, collagen-II and SOX-9 in NPSCs compared with the control, whereas pre-treatment with RS504393 significantly recovered this reduction compared with the 100 ng/ml MCP-1 group (Fig. 4A and B). Through micromass culture, the effect of MCP-1 on chondrogenic NPSC differentiation induced by TGF-β1 was investigated. The weight of the mass decreased significantly upon treatment with MCP-1 compared with the control; however, this effect was significantly reversed following RS504393 treatment compared with the 100 ng/ml MCP-1 group (Fig. 4C). The protein expression levels of aggrecan and collagen-II were significantly decreased following MCP-1 treatment compared with the control, which was significantly reversed by RS504393 compared with the 100 ng/ml MCP-1 group, as confirmed via immunohistochemical analysis (Fig. 4D). These results therefore suggested that MCP-1 may synergistically inhibit chondrogenic NPSC differentiation induced by TGF-β1 via the MCP-1/CCR2 axis.

Discussion

Stem cell therapy has been considered a promising option for disc regeneration (32,33); however, the potential for the long-term survival and biological function of transplanted cells in a harsh microenvironment remains unclear (34). To solve the possible problems of stem cell transplantation, an alternative method is to mobilize endogenous progenitor and stem cells to the damaged sites. As indicated in numerous studies, progenitor cells in stem cell niches in IDD move toward the annular fibrosus and inner parts of the IDD, which may promote IDD repair *in situ* (35,36). During the natural process of healing, affected cells and tissues release a number of cytokines and chemokines to trigger dormant progenitor cells and activate their migration to the injured sites (37). However, endogenous tissue repair in degenerative IDD by targeting of the local microenvironment or the IDD mechanism is poorly understood. The present study explored the role of MCP-1 in the regulation of the migration and differentiation of endogenous stem cells in IDD to investigate IDD regeneration.

A previous study indicated that IDD releases numerous chemokines and cytokines to effectively recruit endogenous stem cells during the repair process (38). As a pair of ligand receptors, the interaction between MCP-1 and CCR2 is important for the migration and homing of stem cells. MCP-1 may mediate the recruitment of monocytes, and regulate the phenotypes of monocytes and lymphocytes, as well as the accumulation of fibrous tissue and vasculogenesis, with extensive biological effects. For example, the chemotactic effect of HConFs mediated by the MCP-1/CCR2 axis was decreased after transdifferentiation into myofibroblasts (39). The MCP-1/CCR-2 axis activates the PI3K/AKT/mTOR signaling pathway leading to HIF-1α-mediated VEGF-A expression (29).The upregulation of MCP-1 promotes a CCR2-dependent profibrotic and inflammatory state, and accelerates the AKI-to-CKD transition (40). Previous studies on MCP-1 in the intervertebral disc have often focused on its role in attracting macrophages to herniated sites or areas with annular tears (41,42). For example, in murine intervertebral

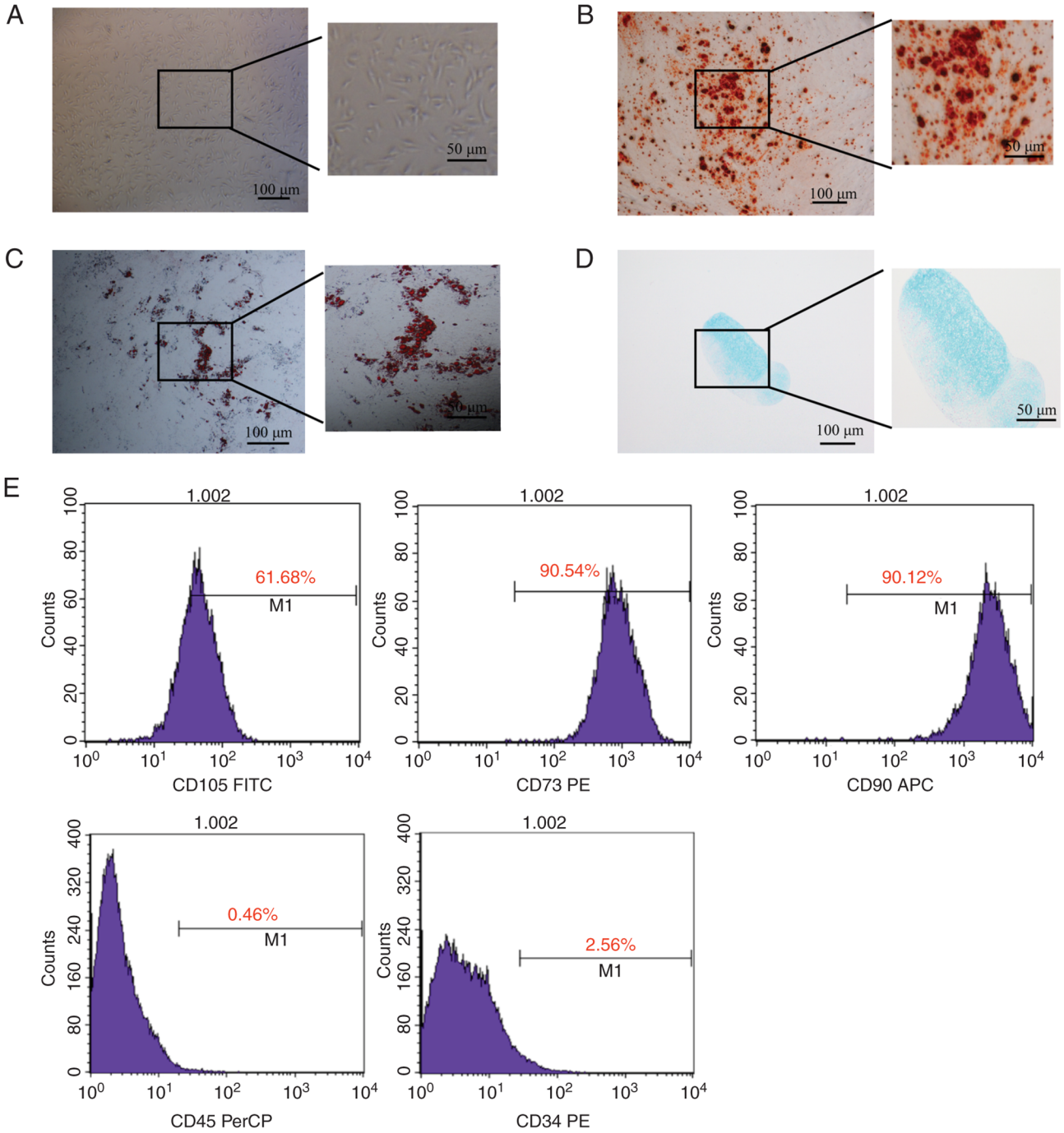

Figure 1. Characterization of NPSCs. (A) P3 generation NPSCs were elongated or fusiform with a clear contour and homogeneous shape (magnification, x100). (B) Osteogenesis-induced Alizarin Red staining revealed red nodules indicative of calcium deposition. (C) Adipogenesis-induced Oil Red O staining demonstrated numerous red areas of lipid droplet vacuolization. (D) Chondrogenesis-induced Alcian Blue staining demonstrated numerous blue areas in cartilage ball sections, suggesting the formation of a large number of cartilage matrices. (E) Flow cytometry of NPSC surface markers revealed low expression of hematopoietic markers CD34 and CD45, and high expression of mesenchymal stem cells markers CD73, CD90 and CD105. NPSC, nucleus pulposus-derived stem cell; PE, phycoerythrin; PerCP, peridinin-chlorophyll-protein; APC, allophycocyanin.

discs, MCP-1 was reported to induce macrophage migration, which was abrogated by the addition of anti-MCP-1 neutralizing antibodies, indicating that MCP-1 may have an effect on the pathogenesis of IDD (25). A previous study demonstrated that MCP-1 may be detected in culture medium after 48 h of culture with mesenchymal stem cells and could enhance their migration (43). However, the roles of MCP-1 in IDD are still poorly understood and whether MCP-1 can promote the repair of IDD remains unclear.

The mechanism of tissue repair is crucial for the normal functioning and integrity of the body, in which tissues and organs are damaged through frequent exposure to mechanical stress. Endogenous mesenchymal stem cells may be mobilized and activated to promote tissue repair as a regenerative cell population (44,45). Mesenchymal stem cells may mutually communicate with other cells in the body and move to damaged sites, which mainly depends on the response to the cell injury signal (46). Mesenchymal stem cells may

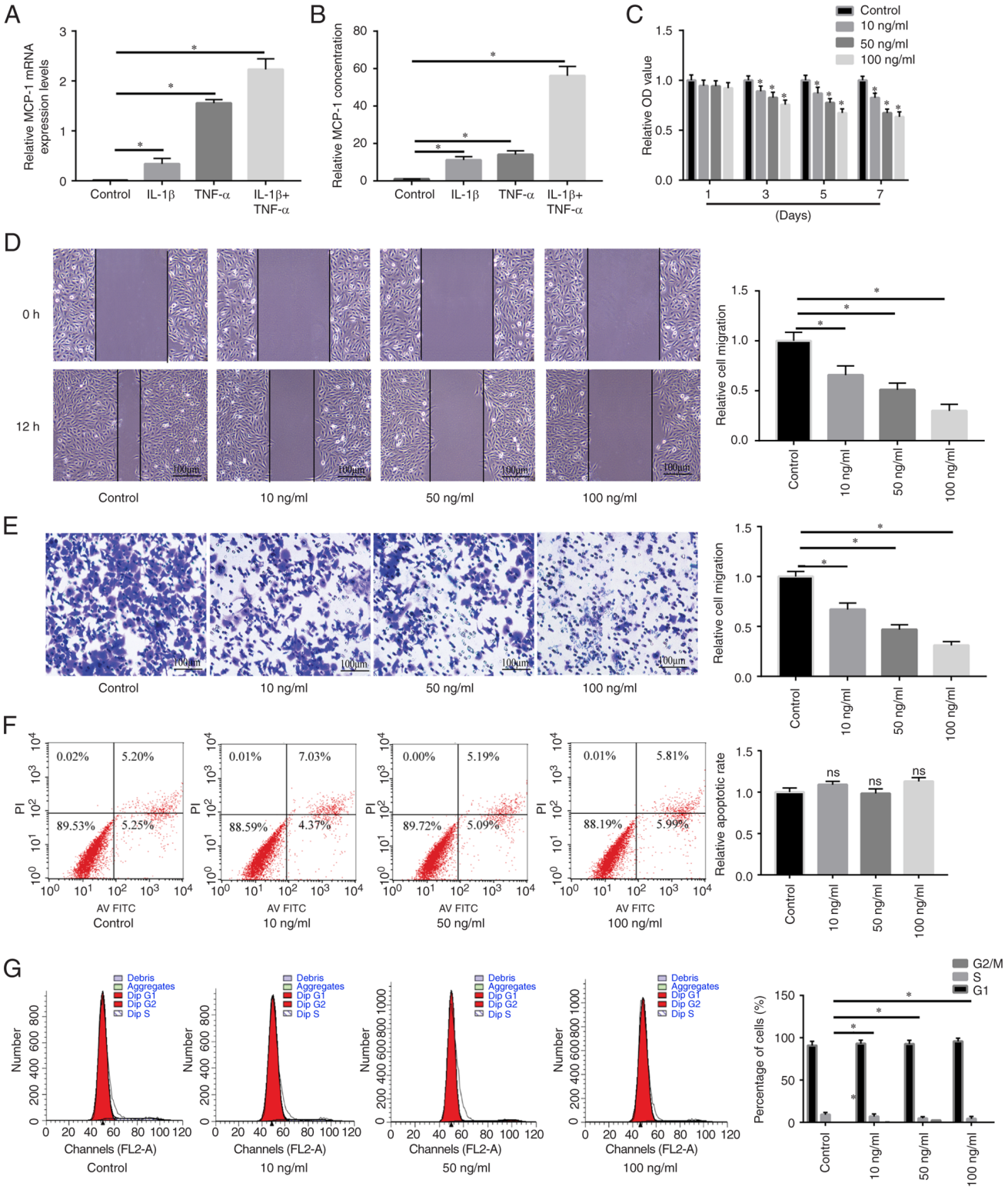

Figure 2. MCP-1 mRNA expression levels and secretion in the intervertebral disc degeneration microenvironment. Reverse transcription-quantitative PCR and ELISA were performed to assess the (A) mRNA expression levels and (B) concentration of stromal cell-derived MCP-1 in NPSCs. MCP-1 expression levels were significantly higher in pro-inflammatory cytokine-treated cells compared with the control. The (C) Cell Counting Kit-8 (D) wound healing and (E) Transwell migration assays determined that the proliferation and migration of NPSCs was dose-dependently significantly suppressed by stromal cell-derived MCP-1. Flow cytometry revealed that MCP-1 did not affect (F) cell apoptosis, but (G) suppressed NPSCs entering into S-G2/M phase in dose-dependent manner. *P<0.05. MCP-1, monocyte chemoattractant protein-1; NPSC, nucleus pulposus-derived stem cell; OD, optical density; AV, Annexin V; PI, propidium iodide.

generate a large amount of cytokines to provide feedback for the transduction of regeneration signals, allowing their mobilization from each site, migration to the target sites and their support of tissue repair (47). The present study demonstrated significantly high expression levels and the release of MCP-1 in native cells *in vitro* under the influence of pro-inflammatory mediators IL-1β and TNF-α. In *in vitro* cell migration and proliferation assays, MCP-1 demonstrated

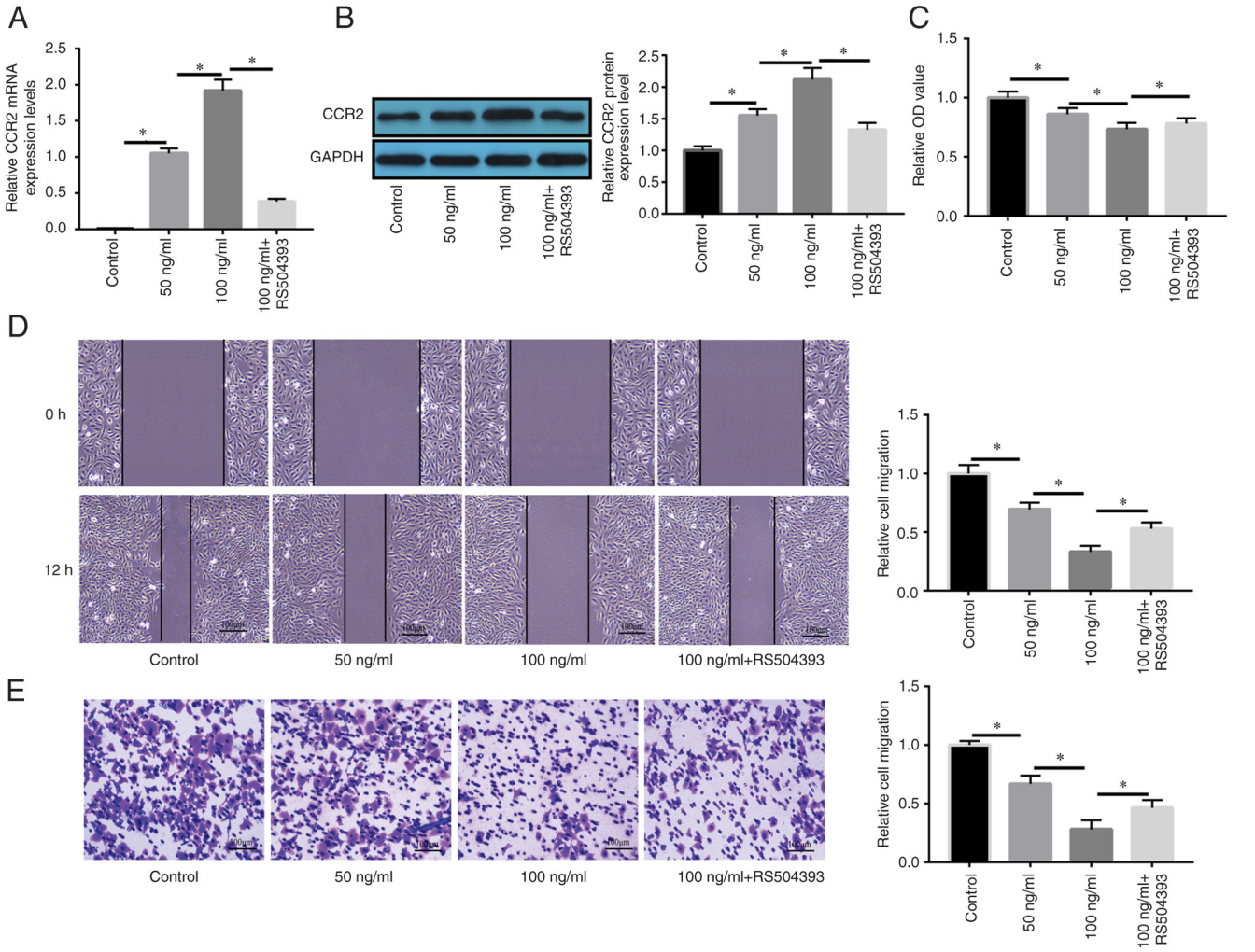

Figure 3. MCP-1/CCR2 axis regulates the proliferation and migration of NPSCs. Following treatment with MCP-1, the (A) mRNA and (B) protein expression levels of CCR2 in NPSCs were significantly increased in a dose-dependent manner; however, this was partially recovered by the CCR2 inhibitor RS504393. (C) CCR2 inhibitor RS504393 partially reversed the suppressive effects of MCP-1 on cell proliferation. (D) RS504393 reversed the suppressive effects of MCP-1 on cell migration partly. (E) The inhibitory effect of MCP-1 on cell migration was partly rescued by RS504393. *P<0.05. MCP-1, monocyte chemoattractant protein-1; CCR2, C-C chemokine receptor type 2; NPSC, nucleus pulposus-derived stem cell; OD, optical density.

a significant dose-dependent inhibitory effect on the migration and proliferation of NPSCs, which indicated that MCP-1 had a regulatory effect on NPSCs. Furthermore, by neutralizing CCR2 with the pharmaceutical inhibitor RS504393, MCP-1 significantly inhibited the proliferation and migration of NPSCs.

Mesenchymal stem cells migrate to inflammatory tissues; however, the specific mechanism of their migration needs to be elucidated further for successful application in clinical settings (48). The recruitment of mesenchymal stem cells is induced via chemotaxis and the directional migration is generated by a concentration gradient. Previous studies have reported that mesenchymal stem cell surfaces express various chemokines and differences in chemokine receptors is most likely caused by differences in isolation techniques and culture conditions (49,50).

The present study demonstrated that MCP-1 significantly upregulated the protein expression levels of its transmembrane receptor CCR2 in NPSCs, possibly to modulate chondrogenic NPSC differentiation upon treatment with TGF-β1. During histological analysis, following micromass culture of NPSCs for chondrogenesis *in vitro*, MCP-1 significantly reduced the weight and size of chondrogenic pellets but also dose-dependently significantly decreased the mRNA and protein expression levels of aggrecan and collagen-II in NPSCs. Conversely, the CCR2 antagonist RS504393 neutralized the inhibitory effect of MCP-1 on chondrogenic NPSC differentiation, as demonstrated by the higher protein expression levels of the chondrogenic markers, SOX-9, collagen-II and aggrecan. These findings suggested that the MCP-1/CCR2 axis may be closely associated with the proliferation and migration of NPSCs, which is essential for the endogenous recruitment of NPSCs. Therefore, the MCP-1/CCR2 axis could be a potential target for the treatment of IDD.

In conclusion, the present study demonstrated a novel mechanism of MCP-1, which accumulated in damaged or degenerative IDD to effectively inhibit chondrogenic NPSC differentiation and migration towards damaged sites via the MCP-1/CCR2 axis. MCP-1 may therefore represent a novel therapeutic target for the regeneration of IDD *in situ* and for endogenous cell repair by targeted inhibition of MCP-1

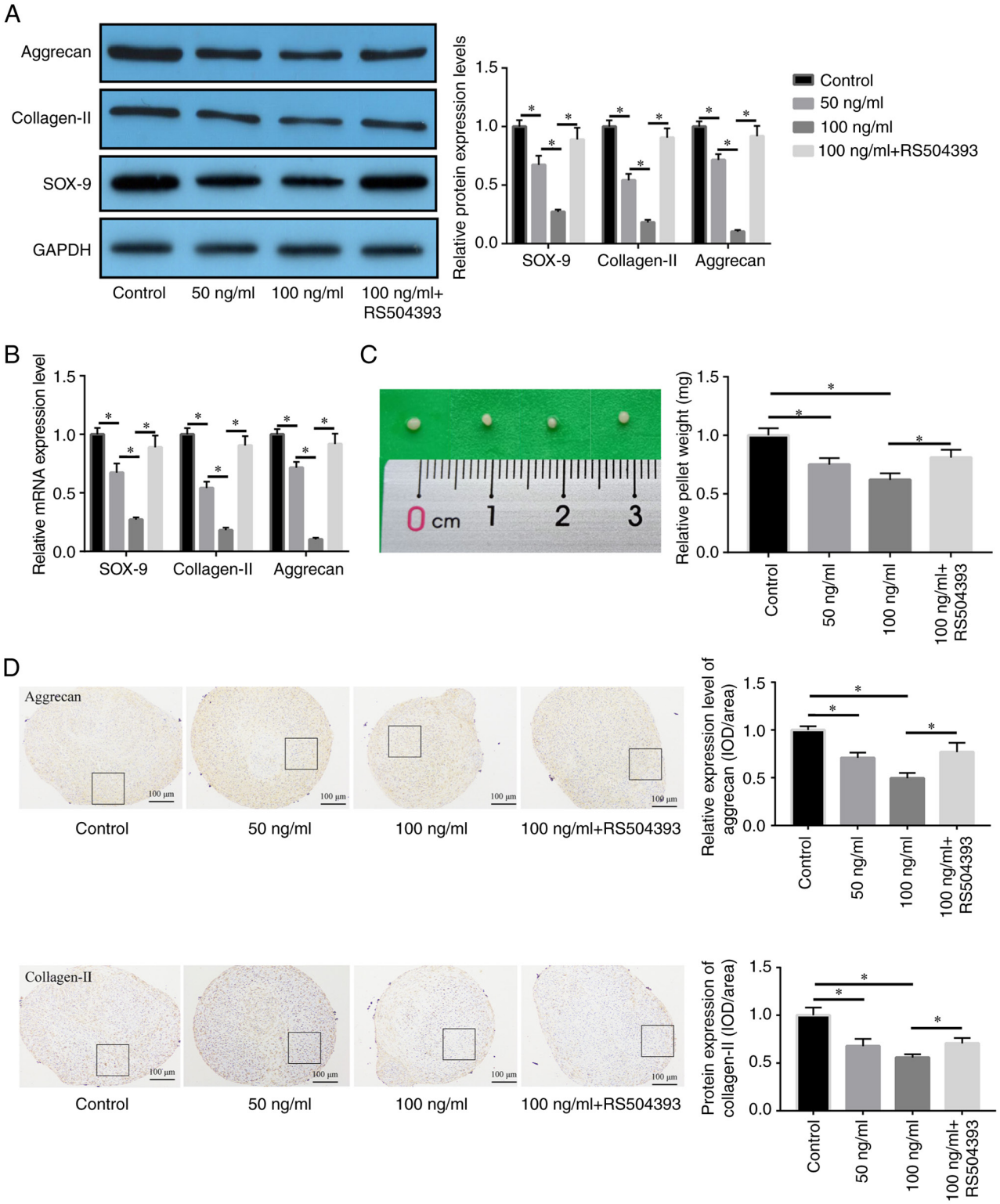

Figure 4. MCP-1/CCR2 axis regulates chondrogenic differentiation of nucleus pulposus-derived stem cells. (A) MCP-1 significantly suppressed chondrogenic differentiation in a dose-dependent manner compared with the control, whereas the CCR2 inhibitor RS504393 significantly reversed the inhibitory effect of MCP-1 compared with the 100 ng/ml group. (B) MCP-1 exhibited a significant dose-dependent upregulation effect on the mRNA expression levels of chondrocyte-related genes/proteins such as Sox-9, collagen-II and aggrecan, compared with the control, which was significantly reversed by RS504393. (C) MCP-1 inhibited chondrogenic differentiation of NPSCs in a dose-dependent manner, but this effect was reversed by RS504393. (D) Immunohistochemical results revealed that MCP-1 significantly inhibited the synthesis and expression of aggrecan and collagen-II in cartilage tissues, which was significantly antagonized by RS504393. *P<0.05. MCP-1, monocyte chemoattractant protein-1; CCR2, C-C chemokine receptor type 2; IOD, integrated optical density.

expression. However, there are still certain limitations to the present study. The downstream signaling pathways of the MCP-1/CCR2 axis remain to be clarified further and *in vivo* experiments are needed to determine the role of MCP-1 in the regulation of numerous biological behaviors of NPSCs in animal systems.

Acknowledgements

Not applicable.

Funding

This work was supported by the National Natural Science Foundation of China (grant no. 81772399).

Availability of data and materials

The datasets used and/or analyzed during the present study are available from the corresponding author on reasonable request.

Authors' contributions

XO and TW performed the experiments and generated data. DR made substantial contributions to the conception and design of the present study. JY, QH and AX conducted data analysis and interpreted the data. XO and DR confirm the authenticity of all the raw data. All authors contributed to the drafting and revision of the manuscript. All authors read, revised and approved the manuscript and agreed to be accountable for all aspects of the research, ensuring the accuracy and integrity of the work.

Ethics approval and consent to participate

The research was approved by the Ethics Committee of The Second School of Clinical Medicine, Southern Medical University (Guangzhou, China; approval nos. ICE2017058 and ICE2017042). Both human and animal ethics approval were received, and the patient's parents provided written consent.

Patient consent for publication

Not applicable.

Competing interests

The authors declare that they have no competing interests.

References

1. Chan WC, Sze KL, Samartzis D, Leung VY and Chan D: Structure and biology of the intervertebral disk in health and disease. Orthop Clin North Am 42: 447-464, 2011.
2. González Martínez E, García-Cosamalón J, Cosamalón-Gan I, Esteban Blanco M, García-Suarez O and Vega JA: Biology and mechanobiology of the intervertebral disc. Neurocirugia (Astur) 28: 135-140, 2017 (In Spanish).
3. Middendorp M, Vogl TJ, Kollias K, Kafchitsas K, Khan MF and Maataoui A: Association between intervertebral disc degeneration and the Oswestry disability index. J Back Musculoskelet Rehabil 30: 819-823, 2017.
4. Liu Y, Li Y, Nan LP, Wang F, Zhou SF, Feng XM, Liu H and Zhang L: Insights of stem cell-based endogenous repair of intervertebral disc degeneration. World J Stem Cells 12: 266-276, 2020.
5. Vinante F and Rigo A: Heparin-binding epidermal growth factor-like growth factor/diphtheria toxin receptor in normal and neoplastic hematopoiesis. Toxins (Basel) 5: 1180-1201, 2013.
6. Gunasekaran A, de Los Reyes NKM, Walters J and Kazemi N: Clinical presentation, diagnosis, and surgical treatment of spontaneous cervical intradural disc herniations: A review of the literature. World Neurosurg 109: 275-284, 2018.
7. Lofrese G, Mongardi L, Cultrera F, Trapella G and De Bonis P: Surgical treatment of intraforaminal/extraforaminal lumbar disc herniations: Many approaches for few surgical routes. Acta Neurochir (Wien) 159: 1273-1281, 2017.
8. Gillet P: The fate of the adjacent motion segments after lumbar fusion. J Spinal Disord Tech 16: 338-345, 2003.
9. May M: Regenerative medicine: Rebuilding the backbone. Nature 503: S7-S9, 2013.
10. Roberts S, Evans H, Trivedi J and Menage J: Histology and pathology of the human intervertebral disc. J Bone Joint Surg Am 88 (Suppl 2): S10-S14, 2006.
11. Wang R, Luo D, Li Z and Han H: Dimethyl fumarate ameliorates nucleus pulposus cell dysfunction through activating the Nrf2/HO-1 pathway in intervertebral disc degeneration. Comput Math Methods Med 2021: 6021763, 2021.
12. Colombier P, Clouet J, Hamel O, Lescaudron L and Guicheux J: The lumbar intervertebral disc: from embryonic development to degeneration. Joint Bone Spine 81: 125-129, 2014.
13. Hughes SP, Freemont AJ, Hukins DW, McGregor AH and Roberts S: The pathogenesis of degeneration of the intervertebral disc and emerging therapies in the management of back pain. J Bone Joint Surg Br 94: 1298-1304, 2012.
14. Sivakamasundari V and Lufkin T: Stemming the degeneration: IVD stem cells and stem cell regenerative therapy for degenerative disc disease. Adv Stem Cells 2013: 724547, 2013.
15. Risbud MV, Guttapalli A, Tsai TT, Lee JY, Danielson KG, Vaccaro AR, Albert TJ, Gazit Z, Gazit D and Shapiro IM: Evidence for skeletal progenitor cells in the degenerate human intervertebral disc. Spine (Phila Pa 1976) 32: 2537-2544, 2007.
16. Blanco JF, Graciani IF, Sanchez-Guijo FM, Muntión S, Hernandez-Campo P, Santamaria C, Carrancio S, Barbado MV, Cruz G, Gutierrez-Cosío S, *et al*: Isolation and characterization of mesenchymal stromal cells from human degenerated nucleus pulposus: Comparison with bone marrow mesenchymal stromal cells from the same subjects. Spine (Phila Pa 1976) 35: 2259-2265, 2010.
17. Zhao Y, Jia Z, Huang S, Wu Y, Liu L, Lin L, Wang D, He Q and Ruan D: Age-related changes in nucleus pulposus mesenchymal stem cells: An in vitro study in rats. Stem Cells Int 2017: 6761572, 2017.
18. Urban JP: The role of the physicochemical environment in determining disc cell behaviour. Biochem Soc Trans 30: 858-864, 2002.
19. Liu ZJ, Zhuge Y and Velazquez OC: Trafficking and differentiation of mesenchymal stem cells. J Cell Biochem 106: 984-991, 2009.
20. Vanden Berg-Foels WS: In situ tissue regeneration: Chemoattractants for endogenous stem cell recruitment. Tissue Eng Part B Rev 20: 28-39, 2014.
21. Wang J, Markova D, Anderson DG, Zheng Z, Shapiro IM and Risbud MV: TNF-α and IL-1β promote a disintegrin-like and metalloprotease with thrombospondin type I motif-5-mediated aggrecan degradation through syndecan-4 in intervertebral disc. J Biol Chem 286: 39738-39749, 2011.
22. Ou X, Ying J, Bai X, Wang C and Ruan D: Activation of SIRT1 promotes cartilage differentiation and reduces apoptosis of nucleus pulposus mesenchymal stem cells via the MCP1/CCR2 axis in subjects with intervertebral disc degeneration. Int J Mol Med 46: 1074-1084, 2020.
23. Ferreira JR, Teixeira GQ, Neto E, Ribeiro-Machado C, Silva AM, Caldeira J, Pereira CL, Bidarra S, Maia AF, Lamghari M, *et al*: IL-1β-pre-conditioned mesenchymal stem/stromal cells' secretome modulates the inflammatory response and aggrecan deposition in intervertebral disc. Eur Cell Mater 41: 431-453, 2021.
24. Cai WT, Guan P, Lin MX, Fu B and Wu B: Sirt1 suppresses MCP-1 production during the intervertebral disc degeneration by inactivating AP-1 subunits c-Fos/c-Jun. Eur Rev Med Pharmacol Sci 24: 5895-5904, 2020.
25. Takayama Y, Ando T, Ichikawa J and Haro H: Effect of thrombin-induced MCP-1 and MMP-3 production via PAR1 expression in murine intervertebral discs. Sci Rep 8: 11320, 2018.
26. Yaghooti H, Mohammadtaghvaei N and Mahboobnia K: Effects of palmitate and astaxanthin on cell viability and proinflammatory characteristics of mesenchymal stem cells. Int Immunopharmacol 68: 164-170, 2019.
27. Cao M, Liu H, Dong Y, Liu W, Yu Z, Wang Q, Wang Q, Liang Z, Li Y and Ren H: Mesenchymal stem cells alleviate idiopathic pneumonia syndrome by modulating T cell function through CCR2-CCL2 axis. Stem Cell Res Ther 12: 378, 2021.

28. Ferland-McCollough D, Maselli D, Spinetti G, Sambataro M, Sullivan N, Blom A and Madeddu P: MCP-1 feedback loop between adipocytes and mesenchymal stromal cells causes fat accumulation and contributes to hematopoietic stem cell rarefaction in the bone marrow of patients with diabetes. Diabetes 67: 1380-1394, 2018.
29. Sun C, Li X, Guo E, Li N, Zhou B, Lu H, Huang J, Xia M, Shan W, Wang B, *et al*: MCP-1/CCR-2 axis in adipocytes and cancer cell respectively facilitates ovarian cancer peritoneal metastasis. Oncogene 39: 1681-1695, 2020.
30. Yadav A, Saini V and Arora S: MCP-1: chemoattractant with a role beyond immunity: A review. Clin Chim Acta 411: 1570-1579, 2010.
31. Livak KJ and Schmittgen TD: Analysis of relative gene expression data using real-time quantitative PCR and the 2(-Delta Delta C(T)) method. Methods 25: 402-408, 2001.
32. Wang HC, Jin CH, Kong J, Yu T, Guo JW, Hu YG and Liu Y: The research of transgenic human nucleus pulposus cell transplantation in the treatment of lumbar disc degeneration. Kaohsiung J Med Sci 35: 486-492, 2019.
33. Iwashina T, Mochida J, Sakai D, Yamamoto Y, Miyazaki T, Ando K and Hotta T: Feasibility of using a human nucleus pulposus cell line as a cell source in cell transplantation therapy for intervertebral disc degeneration. Spine (Phila Pa 1976) 31: 1177-1186, 2006.
34. Wuertz K, Godburn K, Neidlinger-Wilke C, Urban J and Iatridis JC: Behavior of mesenchymal stem cells in the chemical microenvironment of the intervertebral disc. Spine (Phila Pa 1976) 33: 1843-1849, 2008.
35. Sun K, Jing X, Guo J, Yao X and Guo F: Mitophagy in degenerative joint diseases. Autophagy 17: 2082-2092, 2021.
36. Tessier S and Risbud MV: Understanding embryonic development for cell-based therapies of intervertebral disc degeneration: Toward an effort to treat disc degeneration subphenotypes. Dev Dyn 250: 302-317, 2020.
37. Andreas K, Sittinger M and Ringe J: Toward in situ tissue engineering: Chemokine-guided stem cell recruitment. Trends Biotechnol 32: 483-492, 2014.
38. Li Z, Peroglio M, Alini M and Grad S: Potential and limitations of intervertebral disc endogenous repair. Curr Stem Cell Res Ther 10: 329-338, 2015.
39. Tsutsumi-Kuroda U, Inoue T, Futakuchi A, Shobayashi K, Takahashi E, Kojima S, Inoue-Mochita M, Fujimoto T and Tanihara H: Decreased MCP-1/CCR2 axis-mediated chemotactic effect of conjunctival fibroblasts after transdifferentiation into myofibroblasts. Exp Eye Res 170: 76-80, 2018.
40. Xu L, Sharkey D and Cantley LG: Tubular GM-CSF promotes late MCP-1/CCR2-mediated fibrosis and inflammation after ischemia/reperfusion injury. J Am Soc Nephrol 30: 1825-1840, 2019.
41. Schroeder M, Viezens L, Schaefer C, Friedrichs B, Algenstaedt P, Rüther W, Wiesner L and Hansen-Algenstaedt N: Chemokine profile of disc degeneration with acute or chronic pain. J Neurosurg Spine 18: 496-503, 2013.
42. Scuderi GJ, Brusovanik GV, Anderson DG, Dunham CJ, Vaccaro AR, Demeo RF and Hallab N: Cytokine assay of the epidural space lavage in patients with lumbar intervertebral disk herniation and radiculopathy. J Spinal Disord Tech 19: 266-269, 2006.
43. Boomsma RA and Geenen DL: Mesenchymal stem cells secrete multiple cytokines that promote angiogenesis and have contrasting effects on chemotaxis and apoptosis. PLoS One 7: e35685, 2012.
44. Mastrolia I, Foppiani EM, Murgia A, Candini O, Samarelli AV, Grisendi G, Veronesi E, Horwitz EM and Dominici M: Challenges in clinical development of mesenchymal stromal/stem cells: Concise review. Stem Cells Transl Med 8: 1135-1148, 2019.
45. Frenette PS, Pinho S, Lucas D and Scheiermann C: Mesenchymal stem cell: Keystone of the hematopoietic stem cell niche and a stepping-stone for regenerative medicine. Annu Rev Immunol 31: 285-316, 2013.
46. Kang SK, Shin IS, Ko MS, Jo JY and Ra JC: Journey of mesenchymal stem cells for homing: strategies to enhance efficacy and safety of stem cell therapy. Stem Cells Int 2012: 342968, 2012.
47. Augello A, Kurth TB and De Bari C: Mesenchymal stem cells: A perspective from in vitro cultures to in vivo migration and niches. Eur Cell Mater 20: 121-133, 2010.
48. Fan XL, Zhang Z, Ma CY and Fu QL: Mesenchymal stem cells for inflammatory airway disorders: Promises and challenges. Biosci Rep 39: BSR20182160, 2019.
49. Petit I, Jin D and Rafii S: The SDF-1-CXCR4 signaling pathway: A molecular hub modulating neo-angiogenesis. Trends Immunol 28: 299-307, 2007.
50. Humbert P, Brennan MA, Davison N, Rosset P, Trichet V, Blanchard F and Layrolle P: Immune modulation by transplanted calcium phosphate biomaterials and human mesenchymal stromal cells in bone regeneration. Front Immunol 10: 663, 2019.